Krypton $4p$, $4s$, and $3d$ partial photoionization cross sections below a photon energy of 260 eV

J. Tulkki
Laboratory of Physics, Helsinki University of Technology, 02150 Espoo, Finland

S. Aksela and H. Aksela
Deparment of Physics, University of Oulu, 90570 Oulu, Finland

E. Shigemasa and A. Yagishita
Photon Factory, National Laboratory for High Energy Physics, Oho 1-1, Tsukuba-shi, Ibaraki 305, Japan

Y. Furusawa
Department of Science and Technology, Meisei University, Hodokubo, Hini-shi, Tokyo 191, Japan
(Received 29 August 1991)

The photoionization of krypton $4p$, $4s$, and $3d$ subshells has been studied theoretically from the $4p$ threshold and experimentally from the $3d$ threshold up to a photon energy of 260 eV. In converting the measured count rates of the $4p$, $4s$, and $3d$ main photoelectron lines into partial cross sections, we have used recent photoion yield measurements to estimate the contribution of multiple-excitation processes to the total photoabsorption cross section. Theoretical partial cross sections and angular asymmetry parameters have been calculated using the multichannel Dirac-Fock method. Eighteen leading single-excitation channels related to the $4p$, $4s$, $3d$, and $3p$ hole configurations of the final ionic state were included. Relaxation was taken into account by using separately optimized initial- and final-state orbitals and by including all the resulting overlap integrals in the transition amplitudes. The relaxation effect was found to depend strongly on the photon energy in the near-threshold regions. For the $3d$ subshell the relaxation reduces the $3d$ cross section by 35–40 % at the maximum, whereas it is less significant for the $4p$ and $4s$ cross sections.

PACS number(s): 32.80.Fb

I. INTRODUCTION

Photoionization of outer-shell electrons in noble-gas atoms has served as a benchmark for experimental and theoretical methods during the past decade [1, 2]. The total absorption cross sections have been predicted fairly well by calculations, based on the random-phase approximation (RPA) [3], RPA with exchange [4], or relativistic RPA (RRPA) [2].

Instrumental progress in the synchrotron-radiation sources and electron spectrometry as well as new experimental techniques like photoion spectroscopy have made it possible for experimenters to partition the total absorption cross section into partial photoelectron cross sections. It has also become increasingly feasible to determine separately the single-excitation (main line) cross section and the related multiple-excitation (satellite processes, including double ionization) cross sections for a particular subshell. Ion spectroscopy has made it possible to obtain the partial cross section for the shakeoff process, which, because of its continuous intensity distribution, cannot be determined reliably by photoelectron spectroscopy.

With increasing experimental accuracy, discrepancies between theory and experiment have become apparent. This breakdown is largely related to the incomplete treatment of many-electron excitations and relaxation effects in the transition amplitudes. The ordinary RPA gives an estimate for the total subshell cross section without giving detailed information about how it is divided into the satellite and main line cross sections [4]. Near-ionization-threshold satellite processes are energetically forbidden and must be excluded from the calculations before a meaningful comparison between theory and experiment can be done.

While most recent experimental and theoretical works [1, 2] have dealt with multiple-excitation and resonance phenomena at photoionization thresholds the role of relaxation is still not fully understood. Inclusion of relaxation or multiple excitation is difficult *ab initio* in the ordinary RPA although extensions of RPA that account for these processes in somewhat phenomenological way have been worked out [4, 5]. In contrast it has been shown by Kutzner and co-workers [5] and Altun, Kutzner, and Kelly [6] using many-body perturbation theory, and by Tulkki [7], using the multichannel multiconfiguration Dirac-Fock method (MMCDF), that inclusion of relaxation is necessary for an accurate evaluation of valence-shell photoionization cross sections.

According to time-independent scattering theory [8] the transition matrix element of the electron-photon interaction operator must be calculated using wave functions corresponding to the state of the target atom long before (initial ground state) and long after (final relaxed

ionic hole states) the absorption of the photon. Relaxation is thereby taken into account by using final-state orbitals that are optimized for the final ionic state of the absorption process and by including all the overlap integrals resulting from the nonorthogonality between the initial and final orbital sets in the transition amplitude. The use of the relaxed final-state wave function implies that the calculated cross section gives the probability that the ion is in a specific quantum-mechanical eigenstate of the *ionic* Hamiltonian after photoabsorption [8]. In the electron spectroscopic experiment the excited final ionic state is specified (within possible degeneracy) by the kinetic energy of the photoelectron, which together with the incoming photon energy define the energy of the final ionic state. This requires that at the moment of detection the photoelectrons do not interact with the target ion, and that correspondingly the target has to be in a fully relaxed single-hole state. This picture may break down in the threshold region, where the decay of a single-hole state by Auger decay can affect the photoelectron via post-collision interaction [9].

The relation between the above scattering theoretical conditions and the computational methods is especially transparent in the K-matrix formulation [8, 10] used in this work. However, basically all theoretical formulations that are not based on direct time integration of the full Hamiltonian including the photon field, target, and photon-electron interaction make use of the same boundary conditions.

II. EXPERIMENT

In this work we present experimental 4s, 4p, and 3d partial cross sections for the 95- to 260-eV photon energy region. The measurements were carried out using monochromated synchrotron radiation from the 24-m spherical grating monochromator [11] at the beamline 3B of the 2.5-GeV storage ring at the Photon Factory. The photoelectron spectra were measured with a spherical mirror-type electron analyzer at selected photon energies between 95 and 260 eV.

In order to convert the count rates associated with the 4p, 4s, and 3d main photoelectron lines to absolute partial cross sections, a partition method was employed as follows. First, the total absorption cross section, measured by Marr and West [12] was divided into two contributions, (1) the single-excitation cross sections (related to the main 4s, 4p, or 3d photoelectron lines) and (2) the multiple-excitation cross sections (all other processes). The sum of single-excitation cross sections (1) was obtained by subtracting the total multiple-excitation cross section (2), determined by using the photoion measurements of Murakami *et al.* [13] from the total absorpton cross section [12]. The relative intensities of the 3d, 4s, and 4p photoelectron lines were extracted from the measured spectrum using a least-squares-fitting program. After that the total single-excitation cross section was divided into 4p, 4s, and 3d subshell cross sections according to their relative intensities.

The measured 4s, 4p, and 3d cross sections are given in Figs. 1–3, together with the present theoretical results and with earlier experimental data [14, 15]. Since an earlier RPA calculation by Shanthi, Deshmukh, and Manson [16] showed an anomalous maximum in the near-threshold behavior of the $3d_{5/2}$-to-$3d_{3/2}$ branching ratio, we have extracted this ratio from our experimental data and compared it with our multichannel Dirac-Fock calculation in Fig. 4.

III. THEORY AND CALCULATIONS

The theoretical cross sections and angular asymmetry parameters β were calculated using the MMCDF method [7]. For comparison the cross sections were also calculated in the single-channel Dirac-Fock approximation using different ionic potentials for the final state. In the calculations, including relaxation, the cross sections were obtained using separately optimized single-configuration initial and final bound states [17]. The continuum orbitals used in the multichannel or single-channel cross sections were generated by keeping the bound final ionic orbitals frozen. The Lagrangian multipliers were employed in all calculations to obtain a set of orthogonal final-state orbitals. In the calculation of transition am-

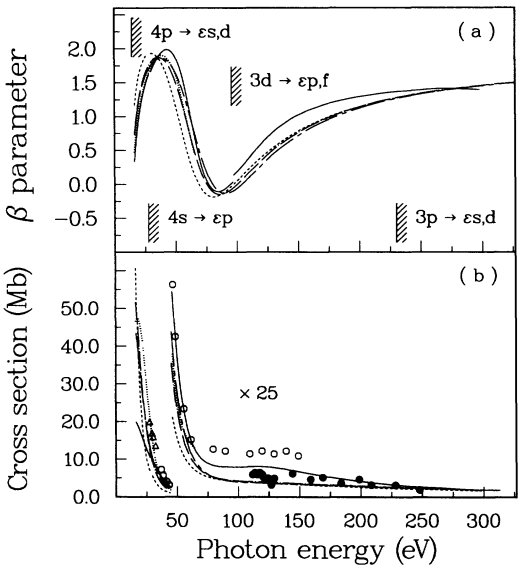

FIG. 1. The krypton 4p partial cross section and the associated asymmetry parameter β. The cross section is a sum of fine-structure components corresponding to the $4p_{1/2}$ and $4p_{3/2}$ hole states and the β parameter represents the weighted average of values obtained for these two components. The fine-structure splitting of ionization energies has been neglected. Theoretical cross sections: solid line, multichannel calculation; dashed line, jj-average single-channel calculation; chain-dashed line, ASF single-channel calculation with relaxation; chain-dotted line, ASF single-channel calculation without relaxation; dotted line, RRPA results (Ref. [2]). The small gaps in the multichannel cross sections and β parameters at ionization thresholds cover the autoionizing-resonance region, which is intentionally excluded in this calculation. Experimental data: solid circles, this work; open circles, previous work [14]; triangles, Samson and Gardner [19].

old for $4p$ and $4s$ subshell ionization and at the maximum of the $3d$ subshell cross section. From a many-body point of view these methods mainly differ at two points. Relaxation is included in our calculation but not in the RRPA, whereas the ground-state and final-ionic-state correlations are approximately included in the RRPA, in contrast to the present calculation.

The effect of relaxation is shown in Figs. 1–3 as a difference between the ASF partial cross sections calculated with (chain-dashed line) and without (chain-dotted) relaxation. Relaxation does not influence the $4p$ and $4s$ cross sections very much, whereas it reduces the $3d$ partial cross section by about 35–40 % at a photon energy of 160 eV. This reduction decreases as a function of photon energy being 15% at 330 eV.

Relaxation and interchannel interaction are not mutually independent many-body effects. Since our ASF calculation neglects interchannel interactions, our estimate of the relaxation effect may be inaccurate at ionization thresholds. For the Xe $5s$ partial cross section it has been shown by Tulkki [7] that the relaxation effect can be very large in the threshold region when the final-state channel interactions are included. In general the relaxation tends to reduce the cross section, because in the calculation of transition amplitudes the one-electron dipole matrix elements are multiplied by overlap factors smaller than 1. In the threshold region the energy dependence of the relaxation effect comes from the interference between several partial amplitudes that contribute to the total transition amplitude. At higher photon energies only the principal amplitude, which in the case of $3d$ includes the $< 3d||D||\epsilon f(p) >$ dipole matrix element multiplied by an overlap factor, is preserved. This corresponds to the sudden approximation limit [20] at which the multiple- to single-excitation cross section ratio is constant. The energy dependence of the relaxation effect in the single-excitation cross section and the energy dependence of the shakeup and shakeoff processes are governed by the same kind of interference effects between partial many-electron transition amplitudes. Therefore our results indicate that there could be an essential energy dependence in the $3d$ shake cross section of about 50–100 eV above the $3d$ cross-section maximum, which is still below the sudden limit. This may explain why the multichannel $3d$ cross section overtakes the experimental one at higher photon energies. At the $3d$ cross-section maximum the present multichannel cross section is clearly below our experimental values.

As can be seen from Figs. 1–3, the inclusion of the interchannel interaction tends to decrease the $3d$ cross section, whereas the $4s$ and $4p$ cross sections increase above the $3d$ threshold. Moreover, all our multichannel cross sections are below experimental results at their respective thresholds. The present calculation neglects the interaction between the $4s^{-1}$ and the double-hole $4p^{-2}4d; J = \frac{1}{2}$ configurations and therefore the calculated $4s$ cross section effectively represents the sum of the $4s$ single-excitation and the corresponding correlation satellite cross sections. According to a separate multiconfiguration Dirac-Fock calculation the intensity ratio of the $4s$ correlation satellites (discrete or continuum) to the main line is $\simeq 1.0$ at asymptotic energies.

It has been shown by Swanson and Armstrong [21] that the krypton $4p$ cross section is strongly influenced by initial-state correlations at threshold. Since these correlations are excluded in the present calculation, the good agreement between our theoretical ASF $4p$ cross sections and experiment at $4p$ threshold may be an artifact resulting from excluding both the channel interactions and the ground-state correlation. Our calculated $4s$ cross section is very close to the RRPA result [2], except at threshold where it is considerably lower.

The earlier photoelectron measurement of the $3d_{5/2}$: $3d_{3/2}$ branching ratio [22] was in pronounced disagreement with theory [16]. In contrast to the RRPA result [16], which exhibits a sharp rise and drop of the branching ratio, the measured ratio was almost constant. In order to verify the earlier results, we have redetermined the branching ratio both experimentally and theoretically. The experimental $3d_{5/2}$: $3d_{3/2}$ branching ratio was determined both from the photoelectron lines and the $M_{4,5}N_1N_{2,3}\,^1P$ Auger electron lines. The branching ratio remains almost constant in the $3d$ ionization region. The experimental ratio increases slightly around 120 eV. Due to the overlap of Auger and photoelectron lines an error limit of 0.05 should be attributed to the experimental values around 120 eV, otherwise the accuracy is 0.02. Our experimental and calculated branching ratios agree rather well, and are also in agreement with previous experimental data.

The angular asymmetry parameter is less sensitive to relaxation. Only in the case of $3d$ is there a larger effect in the near-threshold region, where our ASF cross section excluding relaxation result is close to the RRPA calculation [16], which does not account for relaxation either. The multichannel $4p$ and $3d$ β parameters are in excellent agreement with experiment. Note that the $4s$ β parameter is close to the recent experimental data of Derenbach and Schmidt [23]. In particular, the depth of the dip near the "Cooper minimum" is in good agreement with experimental values, in contrast to the RRPA calculation [2]. However, it is obvious that the coupling between channels related to $4s$ single-hole and $4p^{-2}4d$ double-hole states will make this minimum more shallow in analogy to the behavior of the xenon $5s$ asymmetry parameter [7].

In conclusion, we have shown that photoionization of Kr $4p$, $4s$, and $3d$ electrons is strongly affected both by interchannel interactions and relaxation. The relaxation effect is especially prominent for the $3d$ partial cross section and depends on the excitation energy up to a few hundred eV above threshold, where the sudden approximation becomes valid and relaxation leads to the reduction of the cross section by a constant factor. The remaining discrepancies between experiment and theory are attributed to difficulties in obtaining an accurate evaluation of satellite cross sections, and to the incomplete treatment of correlation effects, in particular to the exclusion of initial and final bound-state correlations and coupling between single- and double-hole ionization channels. On the experimental side it would be particularly useful to measure the dependence of the satellite cross

lation of the amplitudes of $4s$ and $4p$ ionization channels an error is made due to the use of the $3d$ single-hole ionic state. However, the corresponding electrostatic correction terms are included in the residual Hamiltonian, which is later diagonalized in the multichannel continuum space. This cancels very accurately the error included in the calculation of single-channel states. This conclusion was confirmed by auxiliary test calculations that showed that the multichannel cross sections are very independent on a particular valence-shell single-hole state that was chosen to generate the continuum orbitals. This indicates that all these orbital sets effectively define the same function space.

The results of our most elaborate calculations including both relaxation and final-state channel interaction are represented by the solid line in Figs. 1–3. For comparison we have also included RRPA results of Johnson and Cheng [2] and Shanthi, Deshmukh, and Manson [16] (dotted line in Figs. 1–3, dashed line in Fig. 4). The krypton $4p$, $4s$, and $3d$ cross sections have also been calculated by Amusia in the pioneering works on the RPA method [4]. His nonrelativistic cross sections and β parameters are rather close to the RRPA results. This shows that the relativistic effect, which influences the results of the present calculations, mainly via spin-orbit interaction, is rather small.

IV. DISCUSSION

A. Experiment

Our present experimental $3d$ cross section agrees well with the photoion spectroscopy result of Murakami *et al.* [13]. However, since the total multiple-excitation cross section, which is used in the present work for the determination of the sum of single-excitation cross sections, is obtained from the data of Murakami *et al.* [13], these two measurements cannot be considered truly independent.

The present experimental cross sections deviate considerably from our previous experimental cross sections [14] and from the $3d$ cross section of Lindle *et al.* [15]. Note that our present data start just at the threshold of the $3d^{-1}4p^{-1}nl$ process. The difference in the experimental cross sections evidently stems from differences in the evaluation of multiple-excitation cross sections. Since no experimental data for the shake cross section (including shakeoff) were available at the time of previous works, Lindle *et al.* [15] obviously overestimated this contribution. As a consequence they underestimated the single-excitation cross sections. Since the sum of single-excitation cross sections was set equal to the total absorption cross section in our previous work [14] we on the other hand systematically overestimated the individual cross sections. The sum of the $4s$ and $4p$ single-excitation cross sections is lower than the total multiple-excitation cross section in the photon energy range of 120 to 260 eV [13], indicating that a precise determination of the latter cross sections is necessary for an accurate determination of the $3d$, $4p$, and $4s$ single-excitation cross sections. From the ion yield cross sections of Murakami *et al.* [13] we estimate the total shake contribution (including both shakeup and shakeoff) to be 27% of the $3d$ cross section at a photon energy of 170 eV. This figure involves the assumption that all shakeup processes lead to triply ionized ions. Therefore 27% should be taken as a lower limit for the contribution of all shake processes. Murakami *et al.* [13] determined the shake cross section up to 210 eV. In this work we have used the same constant value for photon energies up to 260 eV. In the x-ray excited $3d$ photoelectron spectrum [18] the shakeup contribution was observed to be 8% of the $3d$ main line.

In the present experiment the $4p$ cross section was found to be about 5% and the $4s$ cross section about 1% of the $3d$ cross section at a photon energy of 170 eV. The inaccuracy in the branching ratio of the $3d$, $4s$, and $4p$ cross sections, arising from the spectrometer transmission and subtraction of the Auger lines from the photoelectron lines in the region where they partly overlap, is at least of the order of 1% of the $3d$ cross section. This is of the same order of magnitude as the $4s$ cross section itself. Therefore our previous and present measurements of branching ratios of single-excitation cross sections are in agreement with each other within these error limits.

We have made use of the total absorption cross section of Marr and West [12] when converting the relative cross sections to absolute ones. Murakami *et al.* [13] also normalized their total cross section to that of Marr and West [12] in the photon energy range of 120 to 200 eV. Below the $3d$ threshold, Murakami *et al.* [13], however, obtained 0.465 Mb for the total cross section, which is clearly lower than the value of 0.605 Mb reported by Marr and West [12]. This discrepancy indicates that there is still an essential uncertainty in the experimental cross section that should be kept in mind when comparing experiment with theory.

Between the $4p$ and $3d$ thresholds there are only previous results available [14, 19]. Our previous results [14] were obtained by partitioning the total absorption cross section in accordance with the ratio of intensities of the $4p$ and $4s$ photoelectron lines without subtracting the satellite contribution. The total multiple-excitation cross section is, however, significantly large also in this photon energy range. The x-ray excited spectrum [18] yields a branching ratio of 0.5 between the $4s$ correlation satellites (excluding satellite processes leading to double ionization) and the main line. From the ratio of yields of doubly and singly charged ions below the $3d$ threshold Murakami *et al.* [13] estimated that the total multiple-excitation cross section is at least 72% of the sum of the $4p$ and $4s$ subshell cross sections. This explains, in analogy to the $3d$ case, why our previous valence-shell single-excitation cross sections exceed the theoretical values [14].

B. Theory and comparison

Our theoretical multichannel cross sections and β parameters are in moderate overall agreement both with the experiment and with RRPA calculations of Shanthi, Desmukh, and Manson [16] and Johnson and Cheng [2]. Significant discrepancies between the MMCDF and RRPA cross sections can, however, be found near thresh-

old for $4p$ and $4s$ subshell ionization and at the maximum of the $3d$ subshell cross section. From a many-body point of view these methods mainly differ at two points. Relaxation is included in our calculation but not in the RRPA, whereas the ground-state and final-ionic-state correlations are approximately included in the RRPA, in contrast to the present calculation.

The effect of relaxation is shown in Figs. 1–3 as a difference between the ASF partial cross sections calculated with (chain-dashed line) and without (chain-dotted) relaxation. Relaxation does not influence the $4p$ and $4s$ cross sections very much, whereas it reduces the $3d$ partial cross section by about 35–40 % at a photon energy of 160 eV. This reduction decreases as a function of photon energy being 15% at 330 eV.

Relaxation and interchannel interaction are not mutually independent many-body effects. Since our ASF calculation neglects interchannel interactions, our estimate of the relaxation effect may be inaccurate at ionization thresholds. For the Xe $5s$ partial cross section it has been shown by Tulkki [7] that the relaxation effect can be very large in the threshold region when the final-state channel interactions are included. In general the relaxation tends to reduce the cross section, because in the calculation of transition amplitudes the one-electron dipole matrix elements are multiplied by overlap factors smaller than 1. In the threshold region the energy dependence of the relaxation effect comes from the interference between several partial amplitudes that contribute to the total transition amplitude. At higher photon energies only the principal amplitude, which in the case of $3d$ includes the $< 3d||D||\epsilon f(p) >$ dipole matrix element multiplied by an overlap factor, is preserved. This corresponds to the sudden approximation limit [20] at which the multiple- to single-excitation cross section ratio is constant. The energy dependence of the relaxation effect in the single-excitation cross section and the energy dependence of the shakeup and shakeoff processes are governed by the same kind of interference effects between partial many-electron transition amplitudes. Therefore our results indicate that there could be an essential energy dependence in the $3d$ shake cross section of about 50–100 eV above the $3d$ cross-section maximum, which is still below the sudden limit. This may explain why the multichannel $3d$ cross section overtakes the experimental one at higher photon energies. At the $3d$ cross-section maximum the present multichannel cross section is clearly below our experimental values.

As can be seen from Figs. 1–3, the inclusion of the interchannel interaction tends to decrease the $3d$ cross section, whereas the $4s$ and $4p$ cross sections increase above the $3d$ threshold. Moreover, all our multichannel cross sections are below experimental results at their respective thresholds. The present calculation neglects the interaction between the $4s^{-1}$ and the double-hole $4p^{-2}4d; J = \frac{1}{2}$ configurations and therefore the calculated $4s$ cross section effectively represents the sum of the $4s$ single-excitation and the corresponding correlation satellite cross sections. According to a separate multiconfiguration Dirac-Fock calculation the intensity ratio of the $4s$ correlation satellites (discrete or continuum) to the main line is $\simeq 1.0$ at asymptotic energies.

It has been shown by Swanson and Armstrong [21] that the krypton $4p$ cross section is strongly influenced by initial-state correlations at threshold. Since these correlations are excluded in the present calculation, the good agreement between our theoretical ASF $4p$ cross sections and experiment at $4p$ threshold may be an artifact resulting from excluding both the channel interactions and the ground-state correlation. Our calculated $4s$ cross section is very close to the RRPA result [2], except at threshold where it is considerably lower.

The earlier photoelectron measurement of the $3d_{5/2}$: $3d_{3/2}$ branching ratio [22] was in pronounced disagreement with theory [16]. In contrast to the RRPA result [16], which exhibits a sharp rise and drop of the branching ratio, the measured ratio was almost constant. In order to verify the earlier results, we have redetermined the branching ratio both experimentally and theoretically. The experimental $3d_{5/2}$: $3d_{3/2}$ branching ratio was determined both from the photoelectron lines and the $M_{4,5}N_1N_{2,3}\,^1P$ Auger electron lines. The branching ratio remains almost constant in the $3d$ ionization region. The experimental ratio increases slightly around 120 eV. Due to the overlap of Auger and photoelectron lines an error limit of 0.05 should be attributed to the experimental values around 120 eV, otherwise the accuracy is 0.02. Our experimental and calculated branching ratios agree rather well, and are also in agreement with previous experimental data.

The angular asymmetry parameter is less sensitive to relaxation. Only in the case of $3d$ is there a larger effect in the near-threshold region, where our ASF cross section excluding relaxation result is close to the RRPA calculation [16], which does not account for relaxation either. The multichannel $4p$ and $3d$ β parameters are in excellent agreement with experiment. Note that the $4s$ β parameter is close to the recent experimental data of Derenbach and Schmidt [23]. In particular, the depth of the dip near the "Cooper minimum" is in good agreement with experimental values, in contrast to the RRPA calculation [2]. However, it is obvious that the coupling between channels related to $4s$ single-hole and $4p^{-2}4d$ double-hole states will make this minimum more shallow in analogy to the behavior of the xenon $5s$ asymmetry parameter [7].

In conclusion, we have shown that photoionization of Kr $4p$, $4s$, and $3d$ electrons is strongly affected both by interchannel interactions and relaxation. The relaxation effect is especially prominent for the $3d$ partial cross section and depends on the excitation energy up to a few hundred eV above threshold, where the sudden approximation becomes valid and relaxation leads to the reduction of the cross section by a constant factor. The remaining discrepancies between experiment and theory are attributed to difficulties in obtaining an accurate evaluation of satellite cross sections, and to the incomplete treatment of correlation effects, in particular to the exclusion of initial and final bound-state correlations and coupling between single- and double-hole ionization channels. On the experimental side it would be particularly useful to measure the dependence of the satellite cross

sections on the photon energy in the near-threshold regions.

ACKNOWLEDGMENTS

We thank Professor T. Åberg for a critical reading of the manuscript. We would also like to acknowledge the financial support from the Research Council for the Natural Sciences of the Academy of Finland. We would also like to acknowledge the Japan Ministry of Education, Science and Culture (S.A.) and the Japan Society for Promotion of Science (H.A.) for providing the support that made these experimental studies possible.

[1] For a review on the recent progress in experimental and theoretical photoelectron spectroscopy, see U. Becker, in *The Physics of Electronic and Atomic Collisions*, Proceedings of the 16th International Conference on the Physics of Electronic and Atomic Collisions, New York, 1989, edited by A. Dalgarno, R. S. Freund, P. M. Koch, M. S. Lubell, and T. B. Lucatorto, AIP Conf. Proc. No. 205 (AIP, New York, 1990), p. 162; in *X-ray and Inner-Shell Processes*, Proceedings of the X-90 Conference, Knoxville, 1990, edited by T. A. Carlson, M. O. Krause, and S. T. Manson, AIP Conf. Proc. No. 215 (AIP, New York, 1990), p. 621; H. P. Kelly, *ibid.*; U. Becker and D. A. Shirley, in Proceedings of the 9th International Conference on VUV Physics [Phys. Scr. T**31**, 56 (1990)]; M. Amusia, *ibid.*

[2] W. R. Johnson and K. T. Cheng, Phys. Rev. A **20**, 978 (1979); K.-N. Huang, W. R. Johnson, and K. T. Cheng, At. Data Nucl. Data Tables **26**, 33 (1981).

[3] A. F. Starace, in Encyclopedia of Physics Vol. 31, edited by S. Flügge and W. Mehlhorn (Springer, Berlin, 1982), p. 1.

[4] M. Ya. Amusia, *Atomic Photoeffect* (Plenum, New York, 1990); this reference also describes various modifications and extensions of RPA. In our text RPA refers in general to all these methods.

[5] M. Kutzner, Z. Altun, and H. P. Kelly, Phys. Rev. A **41**, 3612 (1990); M. Kutzner, V. Radojevic, and H. P. Kelly, *ibid.* **40**, 5052 (1989).

[6] Z. Altun, M. Kutzner, and H. P. Kelly, Phys. Rev. A **37**, 4671 (1988).

[7] J. Tulkki, Phys. Rev. Lett. **62**, 2817 (1989); J. Tulkki and T. Åberg, J. Phys. B **18**, L489 (1985). We use the term multichannel-multiconfiguration Dirac-Fock method here, although the ionic final states included in the present calculation are single-configuration hole states.

[8] T. Åberg, Phys. Scr. **21**, 495 (1980); for the basic formulation of the time-independent scattering theory, see N. F. Mott and H. S. W. Massey, *The Theory of Atomic Collisions*, 3rd ed. (Clarendon, Oxford, 1965).

[9] J. Tulkki, G. B. Armen, T. Åberg, B. Crasemann, and M. H. Chen, Z. Phys. D **5**, 241 (1987); G. B. Armen, J. Tulkki, T. Åberg, and B. Crasemann, Phys. Rev. A **36**, 5606 (1987); J. Tulkki, T. Åberg, S. B. Whitfield, and B. Crasemann, *ibid.* **41**, 181 (1990).

[10] K.-N. Huang, Phys. Rev. A **22**, 223 (1980).

[11] A. Yagishita, T. Hayaishi, T. Kikuchi, and E. Shigemasa, Nucl. Instrum. Methods Phys. Res. Sec. A (to be published).

[12] G. V. Marr and J. B. West, At. Data Nucl. Data Tables **18**, 497 (1975).

[13] E. Murakami, T. Hayaishi, A. Yagishita, and Y. Moriska, Phys. Scr. **41**, 468 (1990); T. Hayaishi, A. Yagishita, E. Murakami, E. Shigemasa, Y. Morioka, and T. Sasaki, J. Phys. B **23**, 1633 (1990).

[14] S. Aksela, H. Aksela, M. Leväsalmi, K. H. Tan, and G. M. Bancroft, Phys. Rev. A **36**, 3449 (1987).

[15] D. W. Lindle, P. A. Heimann, T. A. Ferret, P. H. Kobrin, C. M. Truesdale, U. Becker, H. G. Kerkhoff, and D. A. Shirley, Phys. Rev. A **33**, 319 (1986).

[16] N. Shanthi, P. C. Deshmukh, and S. T. Manson, Phys. Rev. A **37**, 4720 (1988).

[17] I. P. Grant, B. J. McKenzie, P. H. Norrington, D. F. Mayers, and N. C. Pyper, Comput. Phys. Commun. **21**, 207 (1980).

[18] S. Svensson, B. Eriksson, N. Mårtensson, G. Wendin, and U. Gelius, J. Electron Spectrosc. **47**, 327 (1988).

[19] J. A. R. Samson and J. L. Gardner, Phys. Rev. Lett. **33**, 671 (1974).

[20] T. Åberg, Ann. Acad. Sci. Fenn. Ser. A6 **308**, 1 (1969).

[21] J. R. Swanson and L. Armstrong, Jr., Phys. Rev A **15**, 661 (1977); *ibid.* **16**, 1117 (1977).

[22] S. Aksela, K. H. Tan, G. M. Bancroft, H. Aksela, B. W. Yates, and L. L. Coastworth, Phys. Rev. A **35**, 1219 (1985).

[23] H. Derenbach and V. Schmidt, J. Phys. B **17**, 83 (1984).